COMPLEX DRIVE MODEL OF LINEAR SYNCHRONOUS MOTOR WITH VARIABLE LOAD

RADOMIR PRUSA

Department of Electric Engineering, Faculty of Mechanical Engineering, Brno University of Technology, Brno, Czech Republic

ROSTISLAV HUZLIK

Department of Electric Engineering, Faculty of Mechanical Engineering, Brno University of Technology, Brno, Czech Republic

RADEK VLACH

Department of Mechatronics, Faculty of Mechanical Engineering, Brno University of Technology, Brno, Czech Republic

DOI: 10.17973/MMSJ.2023_03_2022165

xprusa04@vutbr.cz

This paper compares the results of a real linear synchronous motor and its digital twin. It differs from other common publications in that it uses only basic mathematical models representing a particular physical principle. In this way, a minimum of input parameters was achieved. At the same time, all model input parameters are normally listed in the motor datasheet or are easily measurable. Nowadays, digital twins are very important for the development of new machines. Achieving accuracy using the finite element method is possible, but the time requirement does not allow real-time simulations. The digital twin in this paper is based on a mathematical model involving temperature dependence. The real motor is loaded at different operating points to better evaluate the quality of the model. The structure of the control loops has a significant effect on the response of the digital twin, so the design is based on the motor driver used. The text focuses on linear synchronous motors, but the methods used can be generalized to the plane of rotary synchronous motors.

KEYWORDS

linear synchronous motor, digital twin, thermal analysis, mathematical dynamic model, machine-tool

1 INTRODUCTION

The using of linear motors in production machines is aimed at achieving high movement accuracy. Digital twins, which exhibit responses similar to real machines, can be used to correctly and efficiently design drive control in machines. The enormous advantage of the mentioned design method is to comprehensively process the entire control system in the absence of a real machine.

Based on a review of the available literature, it was found that most of the publications related to modelling deal mainly with the rotating variant of synchronous machines. Solution based on magnetic coenergy presented by [Yin 2019]. Model based on magnetic circuit is described in [Lee 2015]. Publications dealing with linear machines are mostly focused on their control [Abroshan 2008] or [Zhang 2022]. Alternatively, they deal with various design modifications [Xu 2015], [Zhang 2020] or [Fu 2021]. Moreover, when it comes to linear variants, a larger proportion of all topics deal with asynchronous variants ([Sarapulov 2017], [Atiyah 2020] or [Shmakov 2018]) than with synchronous ones.

Furthermore, no publications were found that dealt with the thermal model of a linear machine with respect to position. Alternatively, it would have adjusted the parameters of the thermal model based on this fact. In addition, the vast majority of all thermal models are constructed in a very complex manner and the eventual identification of all heat transfer coefficients cannot be determined from a simple warming test.

2 PROBLEM DEFINITION

As already mentioned, currently there are a number of publications dealing with simulation models of electrical machines that focus on a specific machine type and application such as [Inoue 2015] or [Vacheva 2022]. Next variations of mathematical models of synchronous machines are presented also by a number of publications such as in [Jingnan 2007] or [Xing 2017]. The thermal model of the linear motor solved by the finite element method is presented, for example, in the source [Waindok 2013]. Complex electromechanical model was solved by the authors [Dammers 2001]. The influence of temperature on hysteresis and eddy losses is analysed [Xue 2018].

Focusing only on a specific problem represents a degree of overshadowing of the wider use in other applications. A frequent endeavour of many authors is to accurately model a specific machine or part of a machine, which entails increased demands on computational power and the generation of many input parameters.

Deployment in practical applications is often problematic due to the many input parameters. A good example is the topic of temperature networks, friction models and other topics such as in [Veg 2018], [Palkovic 2012] or [Wang 2022].

In this paper, the development of the model was therefore focused on keeping the number of input parameters as low as possible in order to maintain sufficient quality of the output parameters. Digital twin was created for synchronous linear motor with winding in the primary part (mover) and with permanent magnets in the secondary part (stator). Twin was compared with a real linear motor with same parameters (see Fig. 1).

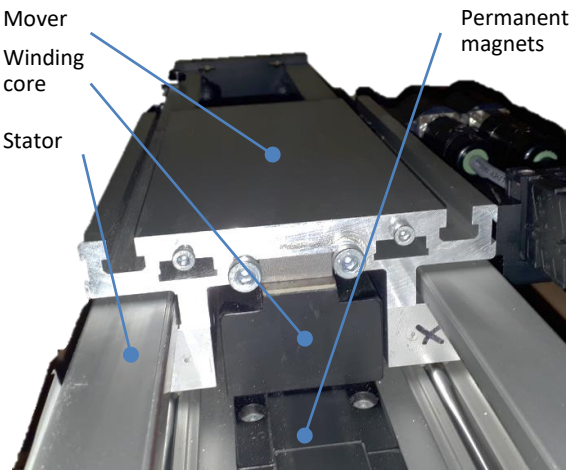

Figure 1. Tested linear synchronous motor

The most common way to model the electromechanical part of the actuator is a model based on the general machine theory, which was developed in the 1930s. Therefore, it may be misleading that reference to older literature will not infrequently be made throughout this article. A suitable example is

[Mericka 1973], where a modelling method is defined by converting an AC three-phase electric machine model to a DC two-phase model. The method in question was chosen because it is widely used in the commercial sphere where it is implemented in servo amplifiers. Last but not least, it is a method that ensures a certain saving of computational capacity compared to an alternating three-phase system.

3 MATHEMATICAL MODEL OF DRIVE WITH LINEAR SYNCHRONOUS MOTOR

3.1 *Electrical and mechanical model of linear motor*

In this paper, the model of motor is based on a linear transformation of a three-phase AC system to a DC two-phase system. The method is known as general machine theory, which implies simplifying conditions: winding is symmetrical three-phase with star connection (without a node), the magnetization characteristic is linear, zero magnetic losses, constant resistance and inductance, constant airgap, none slot effect, the magnetic field in the air gap has a sinusoidal distribution and does not change in the longitudinal axis, marginal effects are not considered [Mericka 1973].

To derive the equations of a linear synchronous machine, conventional equations for a rotary synchronous machine with permanent magnets ware used. Lots of books deal with detailed equations description, such as [Subrt 1987] or [Mericka 1973].

$$\frac{d\Psi_d}{dt} = V_d - Ri_d + \omega_e \Psi_q \tag{1}$$

$$\frac{d\Psi_q}{dt} = V_q - Ri_q - \omega_e(\Psi_d + \Psi_{PM}) \tag{2}$$

$$T_i = \frac{3}{2}\, p\, \Psi_{PM} i_q \tag{3}$$

Equations (1) and (2) description of electric part of machine. Where $d\Psi$ is element of magnetic flux, dt is element of time, V is amplitude of voltage, R is resistance of one winding phase, I is current and ω_e is angular velocity in electric coordinates. Indexes d/q indicates belonging of variable to the axis d or q. Symbol Ψ_{PM} means equivalent magnetic flux from permanent magnets.

Mechanic part is described by equation (3), where T_i is inner torque, p is count of pole pairs.

The difference between the rotary and linear machines consists in only in the mechanical part. Synchronous velocity of linear motors is not depending on number of poles pairs [Gieras 1999]. Therefore, in the case of linear motor number of poles in equations is considered as value 1. The same applies, if setting the initial parameters in commercial inverters i.e. number of pole pairs equal 1 e.g. Control Techniques drivers [Drury 2001]. This reduces the number of variables in the equation. Next can be considered, that inner force F_i is equivalent in linear systems against inner torque T_i in rotary systems by transfer equation (4).

$$F_i = \frac{T_i}{r} \tag{4}$$

Equation (5) for length of circle express variable r.

$$r = \frac{d_m}{2\pi} = \frac{2 \cdot \tau_p}{2\pi} \tag{5}$$

Variable d_m express distance of two neighbouring poles with same magnetization on the secondary part. Parameter is possible express as two times pole pitch τ_p too. Replacing the variable of inner torque in equation (3) by (4) creates equation (6).

$$F_i = \frac{3}{2}\frac{2\pi}{d_m} i_q \Psi_{PM} \tag{6}$$

In practical terms, it is not easy to determine the magnetic flux from rotor permanent magnets. Manufacturers of linear motors as a rule always place so called force constant k_F to their datasheets (e.g. [Siemens 2018] or [Beckhoff 2022]), which is directly related to magnetic flux. Force constant described dependency between inner generated force and effective magnitude of sinusoidal current.

$$F_i = k_F \frac{i_q}{\sqrt{2}} \tag{7}$$

Comparison of equations (6) and (7) gives the resulting dependency between the magnetic flux from permanent magnets and the force constant (8).

$$\Psi_{PM} = k_F \frac{d_m}{3\sqrt{2}\,\pi} \tag{8}$$

In the datasheet, often a voltage constant k_E is given instead of a force constant. The conversion dependence between the two constants is according to the equation (9).

$$k_F = \sqrt{3}\, k_E \tag{9}$$

For describe the linear motion is used the second Newton's law in differential form. The resulting differential equation describing the mechanical part is represented by equation (10).

$$\frac{dv}{dt} = \frac{1}{m}\,(F_i - F_{load}) \tag{10}$$

Where dv is element of linear velocity, m is mass of second (moving) part and F_{load} is outer acting force to system.

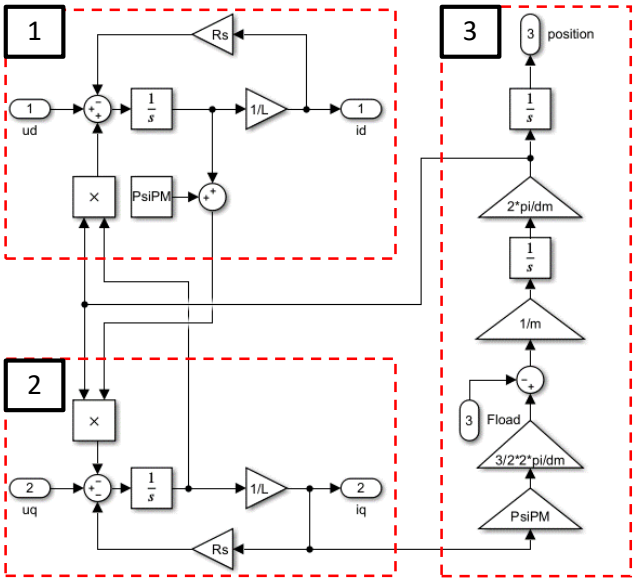

Figure 2. Electrical and mechanical model of linear synchronous motor

System of differential equation was solved by block structure in Matlab Simulink (Fig. 2).

The conversion equation between angular velocity and linear velocity v_e is described by relation (11).

$$\omega_e = v\,\frac{2\pi}{d_m} \tag{11}$$

Magnetic flux in d and q axis is replaced by product induction with current (12).

$$\Psi = L\, i \tag{12}$$

3.2 *Control system*

Control system in this paper has cascade arrangement and consists of three regulators: current, speed and position. Current and speed controller are PI type and position controller is P type.

Model contains current and voltage limitations and switching between maximum torque per ampere control structures and field weakening. Both regulator has proportional and integration component structure (see Fig. 3). The coefficient values used in the control system are shown in the Tab. 1.

Controller type	Value	Unit
Current P	500	[V/A]
Current I	600	[V/A]
Speed P	1	[A/(rad·s^{-1})]
Speed I	5	[A/(rad·s^{-1})]
Position P	300	[(rad·s^{-1})/m]

Table 1. **Parameters of controller loops setup**

Position controller contains only a proportional gain member. Integration and derivative terms are generally not used in position controllers. The reason is to avoid possible overshoots, which in the case of machine tools could lead to damage of the cutting tool (in the case of machine tool). The output of the controller is the angular velocity requirement. The proportional component is situated before the speed saturation.

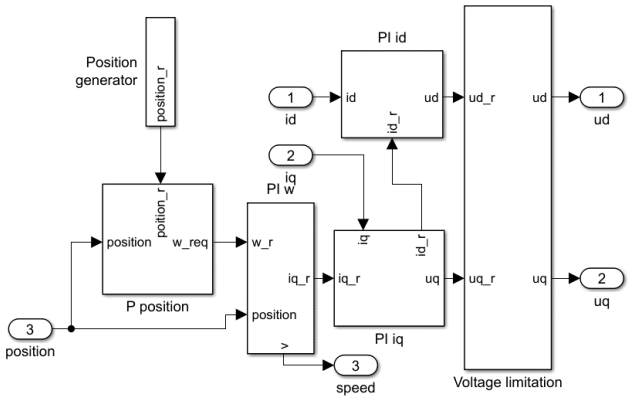

Figure 3 Control system

Trajectory part when mover has zero velocity, winding is still supply by current. These current is called bias current, which holds mover on place with sufficient stiffness against to possible external force. There is constant DC current in each phase with value corresponding to the given mover position. In simulation bias current value was set by coefficient k_{BC} according to parameters in converter (0.5 A was used here). The beginning and end of bias current is derived for position deviation (see Fig. 4). Model structure is based on equation (2).

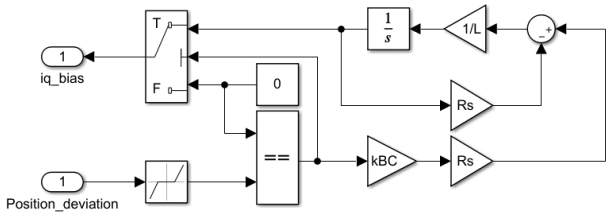

Figure 4. Bias current generator

3.3 *Thermal model of linear motor*

Thermal model is possible created based on complete thermal network with using discrete elements such as [Sarapulov 2017]. This article deals with an asynchronous machine, but from a design point of view, a synchronous machine can also be considered on a macroscopic scale. The difference is in the heat production, specifically in the rotor part. In the case of a synchronous motor, the losses are mainly in the magnets.

This way for practical using of thermal model is not very appropriate, because not all heat transfer coefficients are commonly available for each machine in the datasheets.

According to [Gong 2006], the overall thermal network can be replaced by a single-node network. This particular paper deals with the rotary servo variant. In the linear variant, this simplification takes on a higher potential because the generated heat is only transferred from the windings to the yoke and then directly to the surrounding environment.

The heat transfer from linear motor takes place mainly through the top plate, therefore in the case of water cooling there is here a heat exchanger [Lu 2014].

In electric motor, winding is main heat source and it occurs the greatest warming here. Its maximal warming is limited by insulation class (e.g. 180°C in the case class h or 150°C for f). Therefore the most important temperature is winding temperature T_w. For solve described problem in the case temperature in other parts are not very significant, one nodal thermal network provides sufficient information.

$$R_{th} = \frac{T_w - T_0}{\Delta P_w} \tag{13}$$

The thermal resistance of heat transfer from the windings to the surroundings R_{th} is commonly available or it can be determined based on equation (13). Scheme of one node thermal model is showed in the Fig. 5.

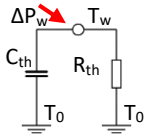

Figure 5. One node thermal model of linear synchronous motor

Equation of one node thermal model is based on thermo-electrical analogy (13). Where ΔP_w represents sum of loss in winding and T_0 is ambient temperature. There is block diagram of the equation Simulink in the Fig. 6.

$$T_w = \int \frac{1}{C_{th}} \cdot \left[\Delta P_w - \frac{T_w - T_0}{R_{th}}\right] \tag{14}$$

The unknown value of the thermal capacity C_{th} is possible determined by equation (15). Warming and cooling curve gives value of thermal time constant τ_{th} [Malousek 1985].

$$\tau_{th} = R_{th} C_{th} \tag{15}$$

Equation was transformed into form of Matlab Simulink structure.

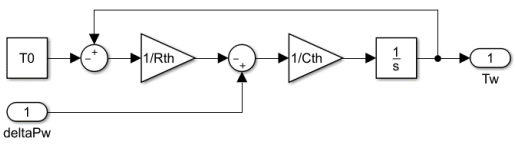

Figure 6. One node thermal simulation model in Simulink

3.4 *Friction model*

The friction model is also a very important part of the whole modelling environment. Without its existence, the measured and simulated results would not match. As in the case of the thermal model, the idea is the same, namely to ensure the

smallest possible number of input parameters. For this reason, the method presented for linear motors, for example in [Kuang 2017], is unacceptable.

The solution is a basic friction model consisting of Coulomb and viscous friction. Where the first type of friction represents the displacement and the second type represents the change in friction magnitude as a function of angular velocity. The values of these two variables can be determined based on the linear line used. The coefficient values used in the friction model are shown in the Tab. 2.

Description	Value	Unit
Coulomb	0.5	[N]
Viscous friction	1.49	[N/[(m·s^{-1})]]

Table 2. **Parameters of friction model**

3.5 *Complete model*

Whole structure can be divide on main several parts: input parameters, electro-mechanic system, thermal system and part with result of simulations (see Fig. 7).

Input parameters are defined in script by coefficients together with measured characteristics. The main idea of model is preserve quality of output parameters with a minimum number of input parameters.

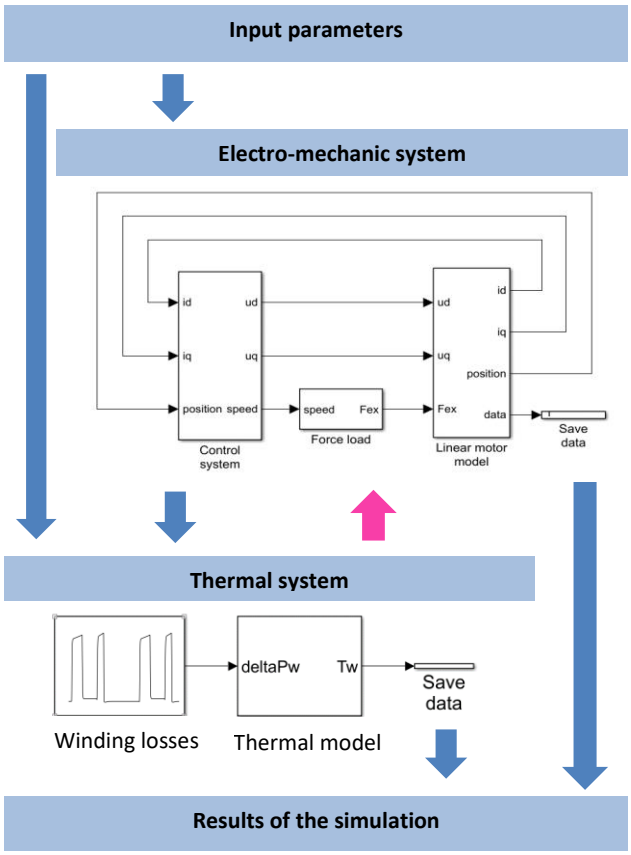

Figure 7. Complete digital twin structure of linear synchronous motor

Complete electro-mechanic system was consisted of two basic building blocks: motor block, control block. Furthermore, there are input blocks, that define the desired positioning and possibly parasitic loads such as friction.

Thermal model builds on previous electro-mechanics system. The most significant sources of heat losses are caused by the passage of current through the winding. To achieve sufficient accuracy at a minimum of variables, other heat losses were neglected.

Due to the significant value difference of thermal and electromechanical time constants calculating progress is separated. The change in winding resistance with temperature is taken into account by iterative calculation between the electromechanical and thermal model.

4 MEASUREMENT OF A LINEAR SYNCHRONOUS MOTOR

The aim of the measurement was a linear synchronous motor type L3S03P-1215-HH (Fig. 1). Temperature class of winding is F. Motor cooling is through the air (without additional water cooler). Winding is three-phase, which is connected into the star. There are parameters in the Tab. 3.

Description	Mark	Value	Unit
Nominal voltage	V_n	400	[V]
Nominal current	I_n	5.8	[A]
Nominal frequency	f_n	200	[Hz]
Nominal force	F_n	300	[N]
Force constant	k_F	60	[N/A]
Winding resistance	R_s	5.6	[Ω]
Inductance	L	31	[mH]
Pole pitch	τ_p	15	[mm]
Mass	m	3,5	[kg]

Table 3. **Parameters of liner synchronous motor L3S03P-1215-HH**

According to key from manufacturing company, motor number (1215) represents other parameters: number of slots (primary part) / number of poles (secondary part) is 12, slot pitch (primary part) / pole pitch (secondary part) is 15 mm.

4.1 *Arrangement of the measuring place*

Measuring place was consisted of from three main parts: linear motor, frequency converter and computer (see Fig. 8). The electrical and mechanical parameters were measured via the integrated driver function. The desired trapezoidal speed profile was set using the PLC program (see Fig. 10). It provided suitable conditions for replicable measurements.

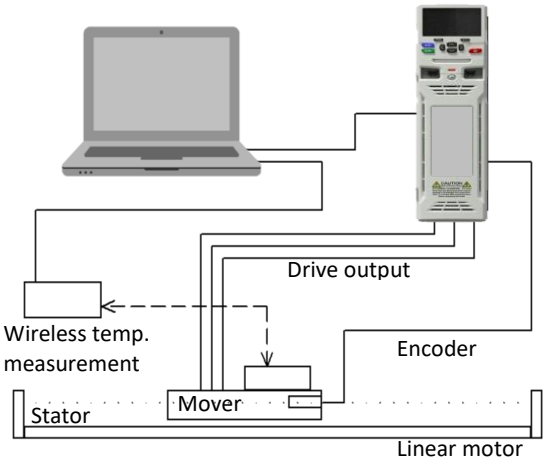

Figure 8. Components of measuring place

The computer was used to set and record selected parameters in time. During experimental measuring was recorded temperature different mover surfaces by wireless sensors. Information about positioning provided a linear magnetic encoder located on the mover. The inductance size for simulation use was based on the inverter measurement.

4.2 *Measured electrical parameters in compare to model*

During the measurements/simulation, the drive performed a cyclic trapezoidal motion according to the S-curve (see Fig. 9). The first graphical dependence shows a comparison of measured and simulated current amplitude. Current peaks (area *a, c*, *e* and *g*) are created in the case acceleration (area *a* and *e*) and deceleration (area *c* and *e*).

Both peaks reach of similar maximal value (maximum was set on 4.5 A), but width is different. These actuality is caused by friction and iron losses, which help slow down of mover.

$$i_A(t) = \sqrt{i_d^2(t) + i_q^2(t)} \tag{16}$$

During constant velocity (area *b* and *f*) current flows only to coverage of friction and iron losses. In the case mover has zero velocity (area *d*), bias current generator is active, therefore total current is not equal to zero (see 2.2). Marked areas in dashed circle with drop peaks are caused by the calculation method of current amplitude (equation 16). Whole course is inverted to the positive part and zero crossing occurs in the places of decline (see Fig. 10).

Small deviations between measurement and simulation can be caused by different control loop settings and inductance sizes.

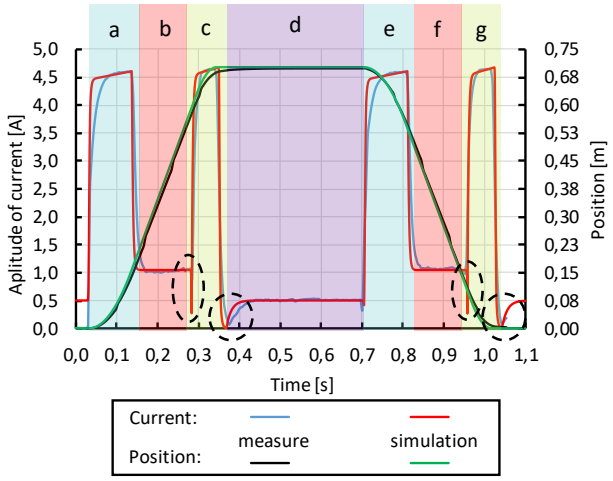

Figure 9. Comparison between measured and simulated parameters: position and current amplitude

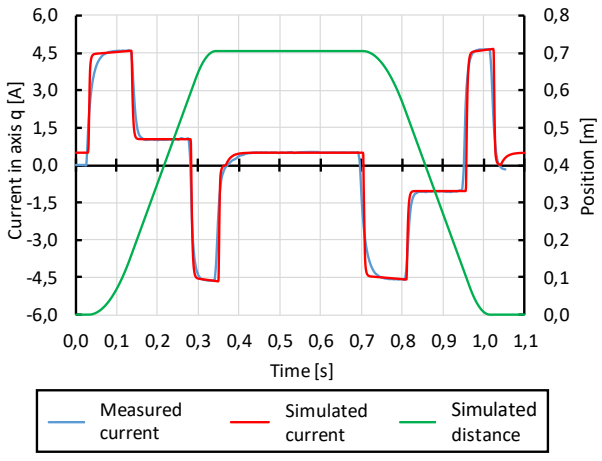

Figure 10. Comparison between measured and simulated current of torque-forming axis

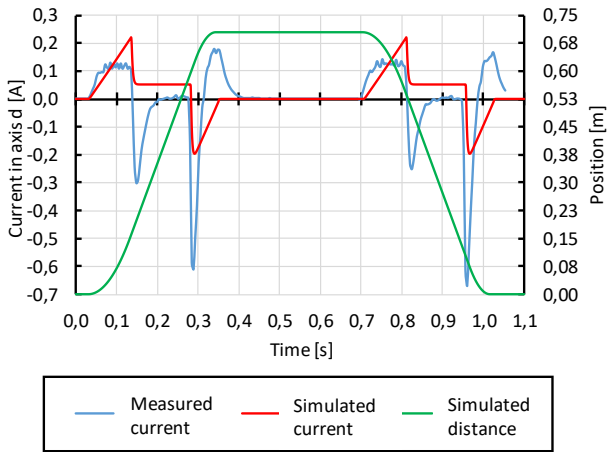

Figure 11. Comparison between measured and simulated current of magneto-forming axis

Converter controls by method maximal torque per ampere (MTPA). Method is based on control structure with zero current level in the d-axis. Same method was set in simulation model. Fig. 10 represents current in axis q (torque-creating axis) and Fig. 11 represents current in axis d (magneto-creating axis). In the case of negative current motor brakes and transmits energy to the inverter braking resistor. It is obvious that the total current is mainly formed by the current in the q-axis (Fig. 9).

The d-axis current is not zero as the MTPA method assumes, this is due to the final speed response of the controllers.

Shape of time power period is similar (Fig. 12). Different is situated in final values. It can be caused different voltage drop on winding impedance (deviation between measure a current state of resistance and inductance).

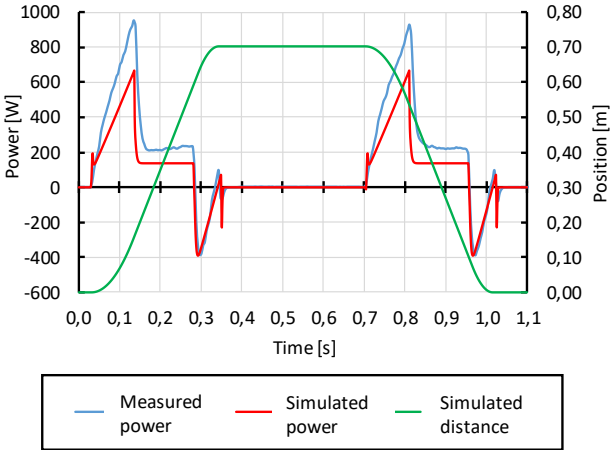

Figure 12. Comparison between measured and simulated input power

4.3 *Temperature conditions*

Thermal model requires two parameters (see Fig. 5): thermal resistance and thermal capacity. Measured machine didn't content built-in winding temperature sensor, therefore it couldn't be direct measuring winding temperature during work cycle.

Temperature monitoring of motor was carried out by two ways. First way was monitoring surface temperatures of difference mover parts and second way was monitoring winding temperature by measuring resistance change of winding. For determination of R_{th} a C_{th}, it can't be use surface warming characteristics. For determination of thermal parameters was used to indirect temperature measurement of winding. Surface

temperatures were used only for orientation measurement and estimation of temperature stabilization.

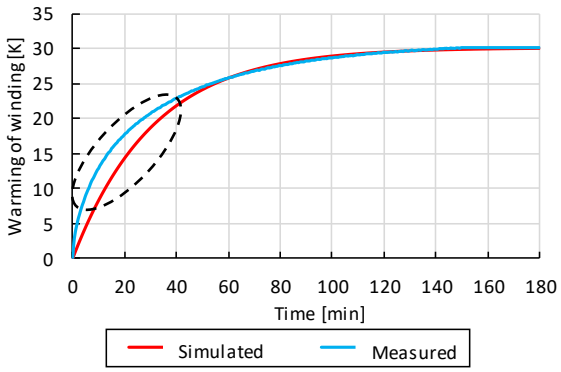

Figure 13. Measured and simulated temperature in winding

First measurement was made in which the mover performed a cyclical duty cycle from one end position to another. The total change in position during one duty cycle was 1400 mm (700 mm in one direction and 700 mm in the other direction). An identical cycle was performed in the previous chapter (Arrangement of the measuring place), which dealt with the time history of current and voltage and power. All control loops, i.e. current, speed and position loops were active during the measurements. The described duty cycle was carried out for the time required for the temperature settling of the machine. The same conditions were also performed in a model environment and the results were then compared.

Fig. 13 shows together simulated and measured curves. Determination of both thermal parameters was based on the measured curve. The measured characteristic lies in this area above the simulated waveform, the reason being the failure to take into account the change in thermal conductivity with temperature. In the case of an actual characteristic, all of the supplied heat is initially stored in the heat capacity and only a small part of the heat passes through the thermal conductivity. As the temperature rises, the thermal conductivity increases and more heat is dissipated. Conversely, in the case of simulation, the magnitude of the thermal conductivity with the temperature is constant and thus a large heat flux escapes even at lower temperatures.

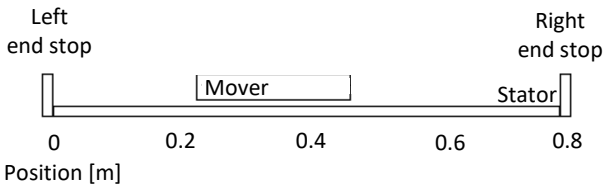

Figure 14. Describing picture for dependency thermal parameters

Linear motor, in contrast to a rotary motor, introduces many variables into the thermal calculation, some of which can significantly affect the deviation as a result, some not. The experimental measurement was carried out five steps. Each step was static measurement (without mover motion) of warming characteristics in which the stator winding was supplied by only a direct current source. The DC power supply was provided by an external stabilized power supply. The inverter was therefore not used in this second thermal measurement. Used value of direct current corresponded to the nominal current according to the Tab. 3. Mover was gradually situated to five position: 0, 0.2, 0.4, 0.6 and 0.8 m (see Fig. 14). In each measured point value of thermal resistance and capacity (one node thermal model) was calculated based on measured warming characteristic (see Fig. 15). The lowest values of both parameters are in the case of the middle position (0.4 m). The closer to the end of the track the two parameters increase (ends are situated on 0 and 0.8 m). Thermal resistance increase due to decrease reduced spontaneous air flow possibilities. The radiation component is also reduced due to the reduction of the effective radiation area. The side of the mover near the end of the track radiates to the end stop and vice versa (total radiant flux is zero).

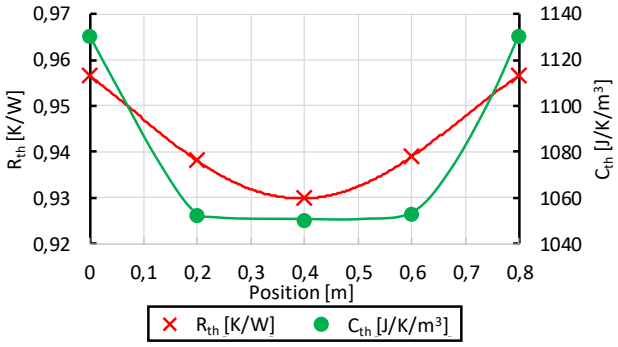

Figure 15. Changing of thermal parameters with mover position

The capacity of the system increases closer to the end of the track due to partial sum material thermal capacity of mover and end stop.

Based on the determined dependence of temperature parameters on the position of the mover, Tab. 4 was created.

Table shows simulation and measuring warming on depending mover position. The power loss in the winding during the trapezoidal motion cycle from the previous part was used as an input value to the simulation. The result is warming, which would be achieved by cyclic movement only in a certain part of the track (i.e. middle, edges, etc.). The table also includes a change in the time constant, which is directly proportional to the change in temperature capacity. It is clear from the results that the position in which the movement is performed also has a certain effect on the final warming, but this dependence is negligible and has not significantly affect the quality of the resulting values.

The simulated and measured values shown in the Tab. 4 can only be compared on the basis of the absolute temperature change at different positions of the path. This is because the simulation included motion and the measurement was static (no motion). In other words, the main purpose of the table is not to compare the measurements and the simulation, but mainly to show the effect of parameter variation on the end temperature.

Table 4. Comparing measurement and simulation thermal parameters in the case different mover position

	Measurement (DC current)			Simulation (Cycling load)	
Position [m]	**ΔP_w [W]**	**ΔT [K]**	**τ [s]**	**ΔP_w [W]**	**ΔT [K]**
0.0	90	86.7	502	32	31.0
0.2		84.4	450		30.4
0.4		83.8	441		30.1
0.6		84.3	449		30.5
0.8		86.8	504		31.0

The methodological procedure was verified on a linear synchronous motor. The whole assembly was in a horizontal position during the measurements. In any case, it can also be generalized for a vertical position or a certain inclination angle. In this case, the temperature parameters of the simplified model will not be symmetrical as in Tab. 4. However, the change of temperature parameters does not need to be addressed for the rotary motor variants. In any case, the simplified temperature model can also be used in the case of a rotating machine form.

5 APPLICATION OF THE MODEL

Due to the specificity of the model, it is necessary to mention its use. The basic idea of the whole modelling was to achieve a minimum of input parameters. Therefore, only basic models that do not contain many detailed parameters were chosen. The presented model can be viewed in terms of methodological approach. An example of an application can be the setup of control structures. First, tuning of the control loops in the model environment is performed to obtain information about the possible motion dynamics. The tuned values of the control constants are then transferred to the real system. By having a simple temperature model, it is also possible to monitor the effect of temperature change on the control quality and adjust the control gain values if necessary.

Furthermore, the effect of the position of the slider on the temperature constants of the temperature model was monitored. If necessary, this finding can be implemented in the model environment so that the temperature model parameters change depending on the position of mover during the execution of a particular cycle.

The text dealt with a linear motor. In the case of machine tools, there are also variants of rotary machines with ball screws. If suitable modifications are made to the dq model, similar principles can be applied to the rotary machine variant.

6 CONCLUSIONS

This paper dealt with comparing between real linear machine and its digital twin. The main idea of created model was preserve quality of output parameters with a minimum number of input parameters. Compared parameters were mainly current, position and input power. The smallest deviations occurred in the case of current. This parameter is very important due to the prediction of control and temperature conditions. Model also solved the so-called bias current, which holds mover on place with sufficient stiffness against possible external force. Deviations of input power was caused by different the voltage drop on winding resistance and inductance. Temperature conditions were solved in this paper too. The change of temperature coefficients depending on the position of the mover was monitored. The change is not significant and changes in the coefficients can be neglected. The ideal choice was a basic single-node thermal network that it has a minimum of parameters and requires low computing power. The resulting simulated warming curve showed lower temperatures in area of exponential increase, which is due to the failure to take into account the change in heat transfer with temperature.

The presented modelling methodology is represented by similar existing models in the Matlab Simulink Simscape Toolbox too. However, these toolboxes are not a standard part of the license. In addition, individual function blocks cannot be modified or look under masks. These are therefore black boxes. The method based on the basic blocks (integration, addition or multiplication) in this paper will ensure modifiability and compatibility with basic software versions. Last but not least, clarity and awareness of internal processes is also ensured. In addition, depending on the specific application, redundant functions can be excluded or, on the contrary, necessary dependencies, non-linearities, etc. can be added.

At first glance, the presented one-node temperature model may seem too simple to be used in real applications. However, in terms of functionality and unambiguous identification of its parameter pairs, it is a very suitable choice for practical deployment. It is only capable of predicting the temperature for a stand-alone motor without external components. On the other hand, this model can be implemented in a more complex temperature model (e.g. of the whole machine tool). In doing so, the parameters of the temperature model will be determined according to a simple measurement and will confidently represent the specific drive.

Virtually every inverter today includes some type of motor temperature model to ensure safe motor operation even during short-term overloads. The difference in the modeling method presented lies in the concept. Due to the easy determination of temperature parameters (heat capacity, thermal resistance) depending on position, the temperature model can be used for adaptive adjustment of the control loop. The model can also be used to predict emergency conditions, where the position of the duty cycle being performed is additionally taken into account. The position disadvantage depends on the axis inclination (horizontal, vertical).

Another research and experimental measurement will be aimed to thermal influence of position sensor and overall thermal influence of other components of the structure for position accuracy (generally of position deviation). Next how to include the prediction of mentioned influences in the case of digital twin and the solution of possible compensations.

The use of these model can be found in many technical applications. These include the prediction of energy requirements for a given duty cycle, the setting of control loops or the simulation of emergency shutdown behaviour. Emergency shutdown, which can occur due to the failure of certain safety features (e.g. optical barriers or limit switches), plays an important role in the safe operation of the machine.

ACKNOWLEDGMENTS

This work is an output of BUT research project Reg. No. FSI-S-20-6335 - Technologie pro digitalni dvojce vyrobnich systemu (Technology for digital twin of production systems).

REFERENCES

[Abroshan 2008] Abroshan, M. and Malekian, K. An optimal direct thrust force control for interior Permanent Magnet Linear Synchronous Motors incorporating field weakening [online]. July 2008. Available from < https://ieeexplore.ieee.org/stamp/stamp.jsp?tp=&arnumber=4581088 >.

[Atiyah 2020] Atiyah, A. and Sulc, B. Role of Asynchronous Motor Modelling in Driven Railway Wheelset Dynamical Simulation Model [online]. Nov 2020. Available from <https://ieeexplore.ieee.org/stamp/stamp.jsp?tp=&arnumber=9257241 >.

[Beckhoff 2022] Documentation: Synchronous servomotors AM8000 & AM8500. Beckhoff, Deutschland, 2022 Available from < https://download.beckhoff.com/download/document/motion/am8000_am8500_ba_en.pdf>.

[Dammers 2001] Dammers, D. and Binet, P. Research of Thermal Regimes of Linear Induction Motor. 2017 18th International Conference on Computational Problems of Electrical Engineering, Santa Rosa, October 2017, Dolphin Integration GmbH, pp 78-83. ISBN 0-7803-7291-3

[Drury 2001] Drury, B. The Control Techniques Drivers and Controls Handbook. IEE, United Kingdom, 2001. ISBN 0-85296-793-4

[Fu 2021] Fu, D. and Si, H. Nonlinear Equivalent Magnetic Network of a Transverse-Flux Permanent Magnet Linear Motor Based on Combine steel with SMC [online]. Aug 2021. Available from <https://ieeexplore.ieee.org/stamp/stamp.jsp?tp=&arnumber=9505982>.

[Gieras 1999] Gieras, J. and Piech, Z. Linear Synchronous Motors: Transportation and Automation Systems. 1999, CRC Press ISBN 08-493-1859-9

[Inoue 2015] Inoue, T. and Inoue, Y. Mathematical Model for MTPA Control of Permanent-Magnet Synchronous Motor in Stator Flux Linkage Synchronous Frame [online]. Mar 2015. Available from <https://ieeexplore.ieee.org/stamp/stamp.jsp?tp=&arnumber=7072549>.

[Jingnan 2007] Jingnan, Z. and Wang, Ch. The Research of Mathematical Model of Six-Phase Double Y-Coil Synchronous Motor Based on Vector Control. 2007 International Conference on Mechatronics and Automation, Harbin, Aug 2007, Harbin Engineering University, pp 2388-2393. ISBN 978-1-4244-0827-6.

[Kuang 2017] Kuang, Z. and Yu, Z. Design of Model-Free Speed Regulation System for Permanent Magnet Synchronous Linear Motor Based on Adaptive Observer [online]. Dec 2017. Available from < https://ieeexplore.ieee.org/stamp/stamp.jsp?tp=&arnumber=8217326>.

[Lee 2015] Lee, K. and Lee, J. Inductance Calculation of Flux Concentrating Permanent Magnet Motor through Nonlinear Magnetic Equivalent Circuit [online]. June 2015. Available from < https://ieeexplore.ieee.org/stamp/stamp.jsp?tp=&arnumber=7113847 >.

[Lu 2014] Lu, Q. and Zhang, X. A Modelling and Investigation of Thermal Characteristics of a Water-Cooled Permanent-Magnet Linear Motor [online]. October 2014, Vol.51, No.3, [September 2019]. Available from https://ieeexplore.ieee.org/stamp/stamp.jsp?tp=&arnumber=6936904&tag=1.

[Malousek 1985] Malousek, A. and Ondruska, E. Ventilation and cooling of the electrical rotating machines. Ostrava, Technical University of Ostrava, 1985.

[Mericka 1973] Mericka, J. and Zoubek, Z. General theory of electric machine. Praha, 1973.

[Palkovic 2012] Palkovic, M. and Makys, P. Influence of static friction and stick-slip phenomena on control quality of SMPM [online]. June 2012. Available from < https://ieeexplore.ieee.org/stamp/stamp.jsp?tp=&arnumber=6225644>.

[Sarapulov 2017] Sarapulov, F. and Sarapulov, S. Research of Thermal Regimes of Linear Induction Motor. 2017 18th International Conference on Computational Problems of Electrical Engineering, Kutna Hora, November 2017, Ural Federal University. ISBN 978-1-5386-1040-4

[Shmakov 2018] Shmakov, L. and Zhang, Z. Design of Model-Free Speed Regulation System for Permanent Magnet Synchronous Linear Motor Based on Adaptive Observer [online]. Mar 2018. Available from <https://ieeexplore.ieee.org/stamp/stamp.jsp?tp=&arnumber=8317204>.

[Gong 2006] GONG, X. and CHEN J. Setup and Implementation of a Simplified Thermal Model for Servomotor. 2006 *2006 IEEE International Symposium on Industrial Electronics*, Móntreal, July 2006. DOI: 10.1109/ISIE.2006.295890.

[Siemens 2018] Configuration manual: Synchronous motors SIMOTCS. Siemens, Nuremberg, 2018, 6SN1197-0AD16-0BP5, Available from https://cache.industry.siemens.com/dl/files/345/55379345/att_68428/v1/1FK7_G2_config_man_0218_en-US.pdf>.

[Subrt 1987] Subrt, J. Electric control drives II. Brno, Brno University of Technology, 1987.

[Vacheva 2022] Vacheva, G. and Dimitrov, V. Mathematical Model of Synchronous Machines for Examination of Energy Flows in Electric Vehicles [online]. Aug 2022. Available from <https://ieeexplore.ieee.org/stamp/stamp.jsp?tp=&arnumber=9845783>.

[Veg 2018] Veg, L. and Laksar, J. Thermal Model of High-Speed Synchronous Motor Created in MATLAB for Fast Temperature Check [online]. Jan 2018. Available from < https://ieeexplore.ieee.org/stamp/stamp.jsp?tp=&arnumber=8624871>.

[Waindok 2013] Waindok, A. Calculation of Temperature in the Permanent Magnet Tubular Linear Motor. 2013 International Symposium on Electrodynamic and Mechatronic Systems, Opole-Zawiercie, May 2013, Opole University of Technology, pp 71-72. ISBN 978-1-4673-5590-2

[Wang 2022] Wang, E. and Grabherr, Z. A Low-Order Lumped Parameter Thermal Network of Electrically Excited Synchronous Motor for Critical Temperature Estimation [online]. Oct 2022. Available from <https://ieeexplore.ieee.org/stamp/stamp.jsp?tp=&arnumber=9910939 >.

[Xing 2017] Xing, S.Ch. and Wang, Ch. Sensorless Control of Three-Phase Permanent Magnet Synchronous Motor Based on Fundamental Wave Mathematical Model. 2017 2nd International Conference on Cybernetics, Robotics and Control, Chengdu, April 2018, University of Chinese Academy of Sciences, pp 89-93. ISBN 978-1-5386-0677-3

[Xu 2015] Xue, S. and Feng, J. Analysis of New Modular Linear Flux Reversal Permanent Magnet Motors [online]. Nov 2015. Available from < https://ieeexplore.ieee.org/stamp/stamp.jsp?tp=&arnumber=7118183>.

[Xue 2018] Xue, S. and Feng, J. A New Iron Loss Model for Temperature Dependencies of Hysteresis and Eddy Current Losses in Electrical Machines [online]. Jan 2018, Vol.54, No.1, [September 2019]. Available from <https://ieeexplore.ieee.org/stamp/stamp.jsp?tp=&arnumber=8168348 >.

[Yin 2019] Yin, LH. and Wu, L. Magnetic Field Prediction in Surface-Mounted PM Machines with Parallel Slot Based on a Nonlinear Subdomain and Magnetic Circuit Hybrid Model [online]. Aug 2019. Available from <https://ieeexplore.ieee.org/stamp/stamp.jsp?tp=&arnumber=8785318>.

[Zhang 2020] Zhang, L. and Zhang, Z. Analysis and Modeling of A Novel Moving-Magnet-Type Linear Synchronous Motor with Ring Structure Winding [online]. Dec 2020. Available from <https://ieeexplore.ieee.org/stamp/stamp.jsp?tp=&arnumber=9291146>.

[Zhang 2022] Zhang, L. and Zhang, Z. Design of Model-Free Speed Regulation System for Permanent Magnet Synchronous Linear Motor Based on Adaptive Observer [online]. June 2022. Available from <https://ieeexplore.ieee.org/stamp/stamp.jsp?tp=&arnumber=9808138>.

CONTACTS:

Ing. Radomir Prusa
Brno University of Technology, Faculty of Mechanical Engineering, Department of Electrical Engineering
Address, Brno, 616 69, Czech Republic
+420 541 142 106, xprusa04@vutbr.cz, www.vutbr.cz

Ing. Rostislav Huzlik, Ph.D.
Brno University of Technology, Faculty of Mechanical Engineering, Department of Electrical Engineering
Address, Brno, 616 69, Czech Republic
+420 541 143 419, huzlik@vutbr.cz, www.vutbr.cz

doc. Ing. Radek Vlach, Ph.D.
Brno University of Technology, Faculty of Mechanical Engineering, Department of Mechatronics
Address, Brno, 616 69, Czech Republic
+420 541 142 860, vlach.r@fme.vutbr.cz, www.vutbr.cz